Contribution from the Department of Chemistry,
University of South Carolina, Columbia, South Carolina 29208

Cluster Synthesis. 21. The Reaction of $Mo_2Ru(CO)_7Cp_2(\mu_3\text{-}S)$ with $Ru(CO)_5$. Synthesis of the First Cluster Complex To Contain Two Quadruply Bridging Carbonyl Ligands.

Richard D. Adams,* James E. Babin, and M. Tasi

Received February 3, 1988

The reaction of $Mo_2Ru(CO)_7Cp_2(\mu_4\text{-}S)$ (**1**) with $Ru(CO)_5$ at 80 °C yields the two higher nuclearity cluster complexes $Mo_2Ru_4(CO)_{13}(\mu_4\text{-}\eta^2\text{-}CO)Cp_2(\mu_4\text{-}S)$ (**2**) and $Mo_2Ru_5(CO)_{14}(\mu_4\text{-}\eta^2\text{-}CO)_2Cp_2(\mu_4\text{-}S)$ (**4**) in the yields 23 and 15%, respectively. Compound **4** was also made from **2** in 47% yield by reaction with $Ru(CO)_5$ at 80 °C. In the absence of $Ru(CO)_5$, **2** isomerizes to the new compound $Mo_2Ru_4(CO)_{14}Cp_2(\mu_4\text{-}S)$ (**3**) at 80 °C in 46% yield. Compounds **2**–**4** were characterized by IR, ^1H NMR, and single-crystal X-ray diffraction analyses. For **2**: space group $P2_1/c$, a = 16.094 (2) Å, b = 11.559 (2) Å, c = 17.420 (3) Å, β = 113.67 (1)°, V = 2968.2 (9) Å^3, Z = 4. The structure was solved by direct methods and was refined (3202 reflections) to the final residual values of R = 0.029 and R_w = 0.029. For **3**: space group $Pbca$, a = 19.210 (6) Å, b = 21.900 (9) Å, c = 13.963 (2) Å, V = 5874 (3) Å^3, Z = 8. The structure was solved by direct methods and was refined (1799 reflections) to the final residual values of R = 0.048 and R_w = 0.046. For **4**: space group $P2_1/m$, a = 13.045 (3) Å, b = 15.308 (4) Å, c = 10.055 (1) Å, β = 111.78 (1)°, V = 1864.4 (7) Å^3, Z = 2. The structure was solved by direct methods and was refined (2161 reflections) to the final residual values of R = 0.040 and R_w = 0.042. The structure of **2** consists of a square-pyramidal Mo_2Ru_3 cluster with a Mo atom in the apical site and a $Ru(CO)_3$ group bridging an Ru–Ru edge of the square base. A quadruply bridging CO ligand (C–O = 1.262 (8) Å, ν(C–O) = 1457 cm^{-1}) is C-coordinated to a $MoRu_2$ triangle of the square pyramid and O-coordinated to the edge-bridging $Ru(CO)_3$ group. The structure of **3** consists of a square-pyramidal $MoRu_4$ cluster with a capping $CpMo(CO)_2$ group. The structure of **4** is similar to that of **2** but has two $Ru(CO)_3$ groups bridging adjacent Ru–Ru edges of the square-pyramidal Mo_2Ru_3 cluster and two quadruply bridging carbonyl ligands that are related by a reflection plane. The quadruply bridging CO ligands are vibrationally coupled and thus exhibit two absorptions (1453 and 1419 cm^{-1}) for the CO stretching vibration. It is proposed that the cluster growth processes involve interactions of $Ru(CO)_4$ fragments generated from $Ru(CO)_5$ with the sulfido ligand in **1** and with the oxygen atoms of the carbonyl ligands in higher nuclearity species.

Introduction

The development of rational syntheses for transition-metal cluster complexes has been one of the most challenging objectives faced by cluster chemists.[1-3] Bridging ligands have been shown to be especially valuable both for promoting the agglomerization of metal-containing groups and for stabilizing the cluster products. Our previous studies have focused on the ability of bridging sulfido ligands to promote cluster condensations and enlargements.[3-8] It is believed that the lone pair of electrons on the sulfido ligand can serve as a site for the initial attachment of a metal-containing grouping M′ to a sulfur-bridged cluster complex A. Recently, we have obtained evidence indicating that (dialkylamino)carbyne ligands B can also promote cluster enlargements.[9]

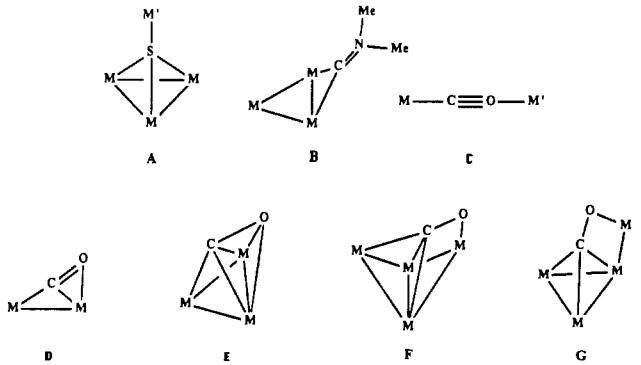

It is well-known that the lone pair of electrons on the oxygen atom of a terminally coordinated carbonyl ligand can form coordinative interactions to Lewis acids C, and there are several well-characterized examples of cluster complexes in which the oxygen atom of a bridging carbonyl ligand is also coordinated to a metal atom.[10]

In this report, the enlargement of the sulfur-containing cluster $Mo_2Ru(CO)_7Cp_2(\mu_3\text{-}S)$ (**1**) by reaction with $Ru(CO)_5$ is described.

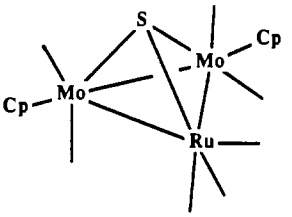

1

The three higher nuclearity clusters $Mo_2Ru_4(CO)_{13}(\mu_4\text{-}\eta^2\text{-}CO)Cp_2(\mu_4\text{-}S)$ (**2**), $Mo_2Ru_4(CO)_{14}Cp_2(\mu_4\text{-}S)$ (**3**) (an isomer of **2**), and $Mo_2Ru_5(CO)_{14}(\mu_4\text{-}\eta^2\text{-}CO)_2Cp_2(\mu_4\text{-}S)$ (**4**) (the first complex to contain two quadruply bridging carbonyl ligands) have been prepared and characterized. Interactions with the carbonyl ligands in the cluster growth process is strongly indicated by the formation of the complexes **2** and **4**, which contain quadruply bridging carbonyl ligands.

Experimental Section

General Data. Although the reaction products are air stable, all reactions were performed under a dry nitrogen atmosphere. Reagent grade solvents were stored over 4-Å molecular sieves. $Mo_2Ru(CO)_7Cp_2(\mu_3\text{-}S)$ (**1**)[11] and $Ru(CO)_5$[12] were prepared by reported procedures. All chromatographic separations were carried out in air. TLC separations were performed on plates (0.25-mm Kieselgel 60 F_{254}, E. Merck) purchased from Bodman Chemicals. IR spectra were recorded on a Nicolet 5DXB FT-IR spectrophotometer. ^1H NMR spectra were run on a Bruker AM-300 spectrometer operating at 300 MHz. Elemental analyses were performed by Desert Analytics, Tucson, AZ.

Reaction of 1 with $Ru(CO)_5$. A 15-mg (0.023-mmol) sample of **1** dissolved in 50 mL of cyclohexane was heated to reflux. A 100-mL

(1) Roberts, D. A.; Geoffroy, G. L. In *Comprehensive Organometallic Chemistry*; Wilkinson, G., Stone, F. G. A., Eds.; Pergamon: Elmsford, NY, 1982; Chapter 40.
(2) Vargas, M. D.; Nicholls, J. N. *Adv. Inorg. Chem. Radiochem.* **1987**, *30*, 123.
(3) Adams, R. D. *Polyhedron* **1985**, *4*, 2003.
(4) Adams, R. D.; Babin, J. E.; Tasi, M. *Organometallics* **1988**, *7*, 503.
(5) Adams, R. D.; Babin, J. E.; Tasi, M. *Inorg. Chem.* **1987**, *26*, 2807.
(6) Adams, R. D.; Babin, J. E.; Tasi, M. *Inorg. Chem.* **1986**, *25*, 4514.
(7) Adams, R. D.; Babin, J. E.; Mahtab, R.; Wang, S. *Inorg. Chem.* **1986**, *25*, 1623.
(8) Adams, R. D.; Horvath, I. H.; Wang, S. *Inorg. Chem.* **1986**, *25*, 1617.
(9) Adams, R. D.; Babin, J. E.; Tanner, J. *Organometallics* **1988**, *7*, 765.
(10) Horwitz, C. P.; Shriver, D. F. *Adv. Organomet. Chem.* **1984**, *23*, 210 and references therein.
(11) Adams, R. D.; Babin, J. E.; Tasi, M. *Organometallics* **1988**, *7*, 219.
(12) Huq, R.; Poë, A. J.; Charola, S. *Inorg. Chim. Acta* **1980**, *38*, 12.

0020-1669/88/1327-2618$01.50/0

Table I. Crystallographic Data for the Structural Analyses of Compounds **2–4**

	2	**3**	**4**
	(A) Crystal Data		
formula	$Ru_4Mo_2SO_{14}C_{24}H_{10}$	$Ru_4Mo_2SO_{14}C_{24}H_{10}$	$Ru_5Mo_2SO_{16}C_{26}H_{10}\cdot 0.5C_6H_6$
temp (±3), °C	23	23	23
space group	$P2_1/c$	*Pbca*	$P2_1/m$
a, Å	16.094 (2)	19.210 (6)	13.045 (3)
b, Å	11.559 (2)	21.900 (9)	15.308 (4)
c, Å	17.420 (3)	13.963 (2)	10.055 (1)
α, deg	90.0	90.0	90.0
β, deg	113.67 (1)	90.0	111.78 (1)
γ, deg	90.0	90.0	90.0
V, Å^3	2968.2 (9)	5874 (3)	1864.4 (7)
M_r	1150.55	1150.55	1346.7
Z	4	8	2
ρ_{calcd}, g/cm^3	2.57	2.60	2.40
	(B) Measurement of Intensity Data		
radiation	Mo Kα (λ = 0.71073 Å)		
monochromator	graphite		
detector aperture, mm: horiz; vert	2.0; 2.0	2.0; 2.0	2.0; 2.0
cryst faces	100, $\bar{1}00$, 11$\bar{1}$, $\bar{1}\bar{1}$1, 1$\bar{1}\bar{1}$, $\bar{1}$11	100, $\bar{1}00$, 010, 0$\bar{1}$0, 01$\bar{1}$, 0$\bar{1}$1, 011, 0$\bar{1}\bar{1}$	1$\bar{1}$0, $\bar{1}$10, 110, $\bar{1}\bar{1}$0, 001, 00$\bar{1}$
cryst size, mm	0.06 × 0.20 × 0.19	0.03 × 0.15 × 0.40	0.11 × 0.16 × 0.18
cryst orientation: direction; deg from ϕ axis	[112]; 24	c^*; 0.8	[102]; 2.6
reflcns measd	$h,k,\pm l$	h,k,l	$h,k,\pm l$
max 2θ	50°	45°	48°
scan type	moving cryst–stationary counter		
ω-scane width:[a] $(A + 0.347 \tan \theta)°$	1.20	1.10	1.10
bkgd (count time at each end of scan)	one-fourth scan time at each end of scan		
ω-scan rate, deg/min	4.0	4.0	4.0
no. of data used ($F^2 \geq 3.0\sigma(F_2)$)	3202	1799	2161
	(C) Treatment of Data		
abs cor coeff, cm^{-1}	empirical	empirical	empirical
	28.7	29.0	26.8
transmission coeff: max; min	1.00; 0.80	1.00; 0.70	1.00; 0.85
P factor	0.02	0.02	0.02
final residuals: R_F; R_{wF}	0.029; 0.029	0.048; 0.046	0.040; 0.042
goodness of fit indicator	1.15	1.25	1.66
largest shift/error value of final cycle	0.00	0.06	0.04
largest peak in final diff Fourier, e/Å^3	0.56	1.01	1.20
no. of variables	406	216	253

[a] Rigaku software uses a multiple-scan technique. If the $I/\sigma(I)$ ratio is less than 10.0, a second scan is made and the results are added to first scan, etc. A maximum of three scans was permitted per reflection.

volume of a cyclohexane solution of $Ru(CO)_5$ (0.23 mmol) was then added dropwise to the refluxing solution of **1** over a period of 1 h while the reaction solution was slowly purged with nitrogen. After the addition, the reaction solution was refluxed for an additional 1 h. The solution was cooled, and the solvent was removed in vacuo. The residue was dissolved in CH_2Cl_2 and was chromatographed by TLC with a hexane/CH_2Cl_2 7/3 solvent mixture to yield 12 mg of $Ru_3(CO)_{12}$, 2.5 mg of green $Mo_2Ru_5(CO)_{14}(\mu_4\text{-}\eta^2\text{-}CO)_2Cp_2(\mu_4\text{-}S)$ (**4**) (15%), 3.4 mg of green $Mo_2Ru_4(CO)_{13}(\mu_4\text{-}\eta^2\text{-}CO)Cp_2(\mu_4\text{-}S)$ (**2**) (23%), and 6.8 mg of unreacted **1**. Yields were calculated on the basis of the amount of **1** consumed in the reaction. For **2**: IR (ν(CO), cm^{-1}, in CH_2Cl_2) 2082 vs, 2049 s, 2017 vs, 2002 s, sh, 1956 m, 1841 m, 1802 w, 1457 w; ^{1}H NMR (δ, in $CDCl_3$) 5.67 (s, 5 H), 5.03 (s, 5 H). Anal. Calcd: C, 25.04; H, 0.86. Found: C, 25.01; H, 0.59. For **4**: IR (ν(CO), cm^{-1}, in CH_2Cl_2) 2090 s, 2073 vs, 2020 vs, 2004 s, sh, 1993 m, 1958 m, 1847 w, 1801 vw, 1453 vw, 1419 w; ^{1}H NMR (δ, in $CDCl_3$) 5.72 (s, 5 H), 5.23 (s, 5 H). Anal. Calcd: C, 25.85; H, 0.97. Found: C, 25.81; H, 0.99.

Reaction of 2 with $Ru(CO)_5$. The reaction of 10 mg (0.009 mmol) of **2** and $Ru(CO)_5$ (0.23 mmol) in refluxing cyclohexane for 3 h was performed as described in the previous section. Separation by TLC resulted in 4.0 mg of **4** (47%), 2.5 mg of unreacted starting material, and 1.1 mg of **3** (14%).

Attempted Reaction of 1 with $Ru_3(CO)_{12}$. A 5.5-mg (0.0084-mmol) sample of **1** and 5.4 mg of $Ru_3(CO)_{12}$ were dissovled in 15 mL of cyclohexane and heated to reflux for 2 h. After this time, IR analysis of the solution showed no evidence of a reaction.

Isomerization of 2. A 8.5-mg (0.0074-mmol) sample of **2** was refluxed in a 30-mL cyclohexane solution for 4 h under a nitrogen atmosphere. TLC separation yielded 1.6 mg of **2** and 3.3 mg of greenish brown $Mo_2Ru_4(CO)_{14}Cp_2(\mu_4\text{-}S)$ (**3**) (46%). For **3**: IR (ν(CO), cm^{-1}, in $CHCl_3$) 2065 s, 2035 s, 2010 vs, 1969 m, 1951 w, sh, 1851 w, 1818 w; ^{1}H NMR (δ, in $CDCl_3$) 5.41 (s, 5 H), 5.28 (s, 5 H). Anal. Calcd: C, 25.04; H, 0.86. Found: C, 25.24; H, 0.45.

Crystallographic Analyses. Opaque dark green crystals of **2** were grown by cooling a solution in a hexane/CH_2Cl_2 9/1 solvent mixture to −20 °C. Opaque dark brown crystals of **3** were grown by slow evaporation of solvent from a solution in benzene solvent at +10 °C. Opaque dark green crystals of **4** were grown from a warm benzene solution by slow cooling to 25 °C. The data crystals were mounted in thin-walled glass capillaries. Diffraction measurements were made on a Rigaku AFC6 automatic diffractometer by using graphite-monochromatized Mo Kα radiation. Unit cells were determined and refined from 25 randomly selected reflections obtained by using the AFC6 automatic search, center, index, and least-squares routines. Crystal data, data collection parameters, and results of the analyses are listed Table I. All data processing was performed on a Digital Equipment Corp. MICROVAX II computer by using the TEXSAN structure-solving program library (version 2.0) obtained from Molecular Structure Corp., College Station, TX. Neutral-atom scattering factors were obtained from the standard sources.[13a] Anomalous dispersion corrections were applied to all non-hydrogen atoms.[13b] Full-matrix least-squares of refinements minimized the function $\sum_{hkl} W(|F_o| - |F_c|)^2$, where $W = 1/\sigma(F)^2$, $\sigma(F) = F_o^2/2F_o$ and $\sigma(F_o^2) = [\sigma(I_{raw})^2 + (PF_o^2)^2]^{1/2}/Lp$.

For **2**, the monoclinic space group $P2_1/c$ was established from systematic absences observed in the data. The structure was solved by a combination of direct methods (MITHRIL) and difference Fourier techniques. All non-hydrogen atoms were refined with anisotropic thermal parameters. The positions of the hydrogen atoms on the cyclopentadienyl rings were calculated by assuming idealized 5-fold geometry and C–H distances of 0.95 Å. The scattering contributions from the hydrogen atoms were included in the structure factor (SF) calculations, but the positions were not refined.

Compound **3** crystallized in the orthorhombic crystal system. The space group *Pbca* was identified from the systematic absences observed in the data during the data collection. The structure was solved by a

(13) *International Tables for X-ray Crystallography*; Kynoch: Birmingham, England, 1975; Vol. IV: (a) Table 2.2B, pp 99–101; (b) Table 2.3.1, pp 149–150.

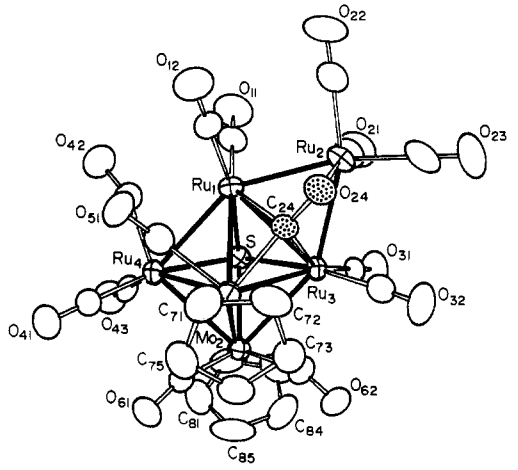

Figure 1. ORTEP diagram of $Mo_2Ru_4(CO)_{13}(\mu_4\text{-}\eta^2\text{-}CO)Cp_2(\mu_4\text{-}S)$ (**2**), showing 50% probability thermal ellipsoids.

combination of direct methods (MITHRIL) and difference Fourier techniques. Due to the limited amount of data, only atoms heavier than oxygen were refined with anisotropic thermal parameters. The positions of the hydrogen atoms on the cyclopentadienyl rings were calculated as described for **2**. Their scattering contributions were added to the SF calculations, but their positions were not refined.

Compound **4** crystallized in the monoclinic crystal system. The absences $0k0$, $k = 2n + 1$, are consistent with either of the space groups $P2_1$ or $P2_1/m$. The latter was chosen initially and confirmed by the successful solution and refinement of the structure. The structure was solved by a combination of direct methods and difference Fourier techniques. The structure contains only half of a formula equivalent of **4** in the asymmetric crystal unit. This is related to the second half by a crystallographic reflection plane. All non-hydrogen atoms were refined with anisotropic thermal parameters. In the final stages of the analysis, a formula equivalent of benzene positioned about a center of symmetry was located. This was added to the analysis and refined with isotropic thermal parameters. Hydrogen atom positions were calculated, and their scattering was added to the SF calculations, but their positions were not refined.

Results

From the reaction of **1** with $Ru(CO)_5$ in cyclohexane solvent at 80 °C, the two new higher nuclearity cluster complexes $Mo_2Ru_4(CO)_{13}(\mu_4\text{-}\eta^2\text{-}CO)Cp_2(\mu_4\text{-}S)$ (**2**) and $Mo_2Ru_5(CO)_{14}(\mu_4\text{-}\eta^2\text{-}CO)_2Cp_2(\mu_4\text{-}S)$ (**4**) were obtained in the yields 23% and 15%, respectively. These compounds were also obtained, but in much lower yields, from the reaction of $Ru_3(CO)_9(\mu_3\text{-}CO)(\mu_3\text{-}S)$ with $Mo_2(CO)_4Cp_2$.[11,14] Compound **4** was obtained from **2** in 47% yield by a further reaction with $Ru(CO)_5$ at 80 °C. When heated to 80 °C for 4 h in cyclohexane, **2** was isomerized to $Mo_2Ru_4(CO)_{14}Cp_2(\mu_4\text{-}S)$ (**3**) in 46% yield. Each of the compounds **2–4** were characterized by IR, ^1H NMR, and single-crystal X-ray diffraction analyses.

Description of the Structure of 2. An ORTEP drawing of the molecular structure of **2** is shown in Figure 1. Final positional parameters are listed in Table II. Intramolecular bond distances and angles are listed in Tables III and IV. The molecule consists of a square-pyramidal cluster of three ruthenium and two molybdenum atoms. Molybdenum Mo1 occupies the apical site of the square pyramid. Molybdenum Mo2 lies in one of the basal positions. The fourth ruthenium atom bridges the Ru1–Ru3 basal edge of the cluster, and the base of the square pyramid is bridged by a quadruply bridging sulfido ligand. The Mo–Mo distance of 3.117 (1) Å is slightly shorter than the Mo–Mo distance of 3.235 (1) Å found in $Mo_2(CO)_6Cp_2$[15] and slightly longer than the Mo–Mo distance of 3.0282 (8) Å found in **1**, but it is very similar to the Mo–Mo distance observed in the square-pyramidal Mo_2Ru_3 cluster of $Mo_2Ru_3(CO)_{10}(\mu\text{-}CO)_2Cp_2(\mu_4\text{-}S)$ (**5**), 3.066 (1) Å (3.110 (1) Å).[11] Except for the long Mo1–Ru1 distance of 3.022

Table II. Positional Parameters and B(eq) for $Mo_2Ru_4(CO)_{13}(\mu_4\text{-}\eta^2\text{-}CO)Cp_2(\mu_4\text{-}S)$ (**2**)

atom	x	y	z	B(eq), Å^2
Ru1	0.77351 (4)	0.08296 (6)	0.31959 (4)	2.58 (3)
Ru2	0.71116 (5)	0.09775 (6)	0.44414 (4)	2.92 (3)
Ru3	0.73727 (4)	−0.11898 (5)	0.39635 (4)	2.18 (2)
Ru4	0.81573 (5)	−0.06339 (6)	0.20920 (4)	2.57 (3)
Mo1	0.63862 (4)	−0.09744 (6)	0.21730 (4)	2.17 (2)
Mo2	0.80065 (5)	−0.26786 (6)	0.29821 (4)	2.35 (3)
S	0.8680 (1)	−0.0871 (2)	0.3604 (1)	2.49 (7)
O11	0.9305 (5)	0.2282 (7)	0.4301 (5)	6.5 (4)
O12	0.6772 (5)	0.3056 (6)	0.2476 (4)	5.7 (4)
O21	0.8939 (5)	0.0861 (7)	0.5855 (4)	6.0 (3)
O22	0.7156 (5)	0.3596 (6)	0.4579 (5)	6.1 (4)
O23	0.6151 (6)	0.0607 (7)	0.5610 (5)	7.4 (4)
O24	0.5913 (4)	0.0667 (5)	0.3340 (3)	3.2 (2)
O31	0.8737 (4)	−0.1906 (6)	0.5676 (4)	4.8 (3)
O32	0.5762 (4)	−0.1930 (6)	0.4306 (4)	4.9 (3)
O41	0.7387 (6)	−0.0917 (6)	0.0213 (4)	6.3 (4)
O42	0.8569 (5)	0.1860 (6)	0.1870 (5)	5.6 (3)
O43	1.0001 (5)	−0.1375 (6)	0.2178 (4)	5.2 (3)
O51	0.6382 (4)	0.1092 (5)	0.1032 (4)	4.3 (3)
O61	0.7037 (4)	−0.3122 (5)	0.1089 (3)	3.7 (3)
O62	0.6414 (4)	−0.3692 (5)	0.3318 (4)	3.8 (3)
C11	0.8710 (7)	0.1711 (8)	0.3876 (6)	3.9 (4)
C12	0.7137 (6)	0.2208 (8)	0.2747 (5)	3.4 (4)
C21	0.8261 (7)	0.0907 (9)	0.5309 (6)	4.2 (4)
C22	0.7086 (6)	0.2630 (9)	0.4512 (5)	3.9 (4)
C23	0.6511 (7)	0.0749 (9)	0.5182 (6)	4.7 (5)
C24	0.6360 (5)	0.0035 (7)	0.3053 (5)	2.3 (3)
C31	0.8212 (6)	−0.1634 (7)	0.5040 (5)	2.7 (3)
C32	0.6385 (6)	−0.1635 (8)	0.4204 (5)	3.4 (4)
C41	0.7686 (6)	−0.0807 (7)	0.0924 (5)	3.6 (4)
C42	0.8360 (6)	0.1022 (8)	0.2063 (6)	3.7 (4)
C43	0.9313 (6)	−0.1108 (7)	0.2167 (5)	3.3 (4)
C51	0.6550 (6)	0.0336 (8)	0.1523 (5)	3.4 (4)
C61	0.7343 (5)	−0.2754 (7)	0.1772 (5)	2.8 (3)
C62	0.6947 (6)	−0.3078 (7)	0.3234 (5)	3.2 (4)
C71	0.4963 (6)	−0.0652 (8)	0.1126 (5)	3.7 (4)
C72	0.4837 (5)	−0.0872 (8)	0.1855 (6)	3.8 (4)
C73	0.5107 (6)	−0.2021 (8)	0.2089 (5)	3.4 (4)
C74	0.5397 (5)	−0.2496 (8)	0.1508 (5)	3.3 (3)
C75	0.5313 (6)	−0.1666 (9)	0.0904 (5)	3.7 (4)
C81	0.9015 (8)	−0.389 (1)	0.2739 (7)	5.3 (5)
C82	0.9477 (7)	−0.3392 (8)	0.3523 (8)	4.9 (5)
C83	0.9100 (8)	−0.3738 (9)	0.4048 (6)	4.8 (5)
C84	0.8399 (8)	−0.4492 (9)	0.3633 (8)	5.2 (5)
C85	0.8340 (7)	−0.4564 (8)	0.2809 (8)	5.5 (5)

Table III. Intramolecular Distances (Å) for $Mo_2Ru_4(CO)_{13}(\mu_4\text{-}\eta^2\text{-}CO)Cp_2(\mu_4\text{-}S)$ (**2**)

Ru1–C11	1.85 (1)	Ru4–Mo1	2.937 (1)
Ru1–C12	1.864 (9)	Mo1–C24	1.940 (8)
Ru1–C24	2.315 (7)	Mo1–C51	1.971 (9)
Ru1–S	2.412 (2)	Mo1–C71	2.315 (8)
Ru1–Ru2	2.737 (1)	Mo1–C72	2.330 (8)
Ru1–Ru4	2.841 (1)	Mo1–C75	2.333 (8)
Ru1–Ru3	2.864 (1)	Mo1–C73	2.341 (8)
Ru1–Mo1	3.022 (1)	Mo1–C74	2.343 (8)
Ru2–C21	1.86 (1)	Mo1–Mo2	3.117 (1)
Ru2–C23	1.92 (1)	Mo2–C61	1.946 (8)
Ru2–C22	1.92 (1)	Mo2–C62	1.978 (9)
Ru2–O24	2.136 (5)	Mo2–C85	2.29 (1)
Ru2–Ru3	2.725 (1)	Mo2–C81	2.31 (1)
Ru3–C32	1.87 (1)	Mo2–C82	2.32 (1)
Ru3–C31	1.889 (9)	Mo2–C83	2.328 (9)
Ru3–C24	2.259 (8)	Mo2–C84	2.346 (9)
Ru3–S	2.452 (2)	Mo2–S	2.403 (2)
Ru3–Mo2	2.885 (1)	Ru1–C51	2.827 (9)
Ru3–Mo1	2.887 (1)	Ru4–C51	2.621 (9)
Ru4–C41	1.874 (9)	Ru1–C42	2.559 (9)
Ru4–C43	1.89 (1)	Ru4–C61	2.729 (9)
Ru4–C42	1.95 (1)	Ru3–C62	2.480 (9)
Ru4–S	2.438 (2)	C24–O24	1.262 (8)
Ru4–Mo2	2.890 (1)		

(14) Adams, R. D.; Babin, J. E.; Tasi, M. *Angew Chem., Int. Ed. Engl.* **1987**, *26*, 685.
(15) Adams, R. D.; Collins, D. E.; Cotton, F. A. *Inorg. Chem.* **1974**, *13*, 1086.

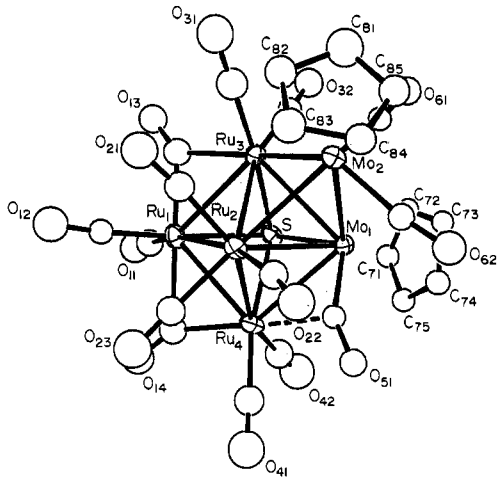

Figure 2. ORTEP diagram of $Mo_2Ru_4(CO)_{14}Cp_2(\mu_4\text{-}S)$ (**3**), showing 50% probability thermal ellipsoids.

(1) Å, all the Mo–Ru distances are very similar in length, 2.885 (1)–2.937 (1) Å. The latter are similar to the Mo–Ru distances found in **1** and **5**, although in **5** the apical–basal Mo–Ru bonds

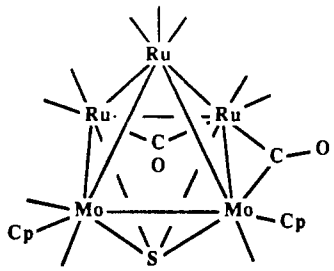

5

were significantly longer than the basal–basal Mo–Ru bonds.[11] The Ru–Ru bonds in the square pyramid, 2.841 (1) and 2.864 (1) Å, are significantly longer than those to the bridging atom Ru2, 2.737 (1) and 2.725 (1) Å. The former are also significantly longer than the CO-bridged Ru–Ru bond, 2.756 (1) Å (2.796 (1) Å), in **5**. The metal–sulfur bonds in **2** are very similar to those in **5**.

Compound **2** contains 14 carbonyl ligands. Nine of these are of a linear terminal type. Four others, C42–O42, C51–O51, C61–O61, and C62–O62, adopt semibridging modes, and of these, C51–O51 could be viewed as a semitriple bridge with a primary bonding to Mo1 and weak interactions to Ru1, 2.827 (9) Å, and Ru4, 2.621 (9) Å. The most interesting carbonyl ligand is C24–O24, which is a η^2 quadruply bridging ligand that is bonded by its carbon atom to Mo1, Ru1, and Ru3. The Ru2···C24 distance of 2.480 (8) Å could be indicative of a weak bonding interaction to that metal atom also. The oxygen atom O24 is strongly bonded to Ru2, Ru2–O24 = 2.136 (5) Å. Quadruply bridging CO ligands of this type F have been observed previously.[10] Elongation of the C–O bond is a characteristic feature of this bonding mode, and such is the case in **2** also, C24–O24 = 1.262 (8) Å. This bond weakening is usually accompanied by a lowering of the CO bond stretching vibrational frequency.[10] In accord with this, a weak absorption, observed at 1457 cm^{-1} is assigned to this vibration. The η^5-cyclopentadienyl ligands coordinated to the molybdenum atoms exhibit no unusual bonding distortions.

Assuming that the quadruply bridging carbonyl ligand serves as a four-electron donor, compound **2** contains a total of 90 cluster valence electrons. This is the number that is predicted by the polyhedral skeletal electron pair (PSEP) theory for an edge-bridged octahedron in which one of the cluster atoms is a main-group element (i.e. the sulfur atom).[16]

(16) Mingos, D. M. P. *Acc. Chem. Res.* **1984**, *17*, 311.

Table IV. Intramolecular Bond Angles (deg) for $Mo_2Ru_4(CO)_{13}(\mu_4\text{-}\eta^2\text{-}CO)Cp_2(\mu_4\text{-}S)$ (**2**)

C11–Ru1–Ru2	86.8 (3)	O12–C12–Ru1	179.7 (9)
C11–Ru1–Ru4	113.0 (3)	O21–C21–Ru2	177.3 (9)
C11–Ru1–Ru3	115.5 (3)	O22–C22–Ru2	174 (1)
C11–Ru1–Mo1	169.5 (3)	O23–C23–Ru2	179 (1)
C12–Ru1–Ru2	89.2 (3)	O24–C24–Mo1	149.1 (6)
C12–Ru1–Ru4	116.7 (3)	O24–C24–Ru3	116.8 (5)
C12–Ru1–Ru3	136.4 (3)	O24–C24–Ru1	113.6 (5)
C12–Ru1–Mo1	102.4 (3)	Mo1–C24–Ru3	86.5 (3)
C24–Ru1–Ru2	58.1 (2)	Mo1–C24–Ru1	90.0 (3)
C24–Ru1–Ru4	99.7 (2)	Ru3–C24–Ru1	77.5 (2)
C24–Ru1–Ru3	50.3 (2)	O31–C31–Ru3	177.7 (7)
C24–Ru1–Mo1	39.9 (2)	O32–C32–Ru3	176.1 (8)
S–Ru1–Ru2	101.87 (5)	O41–C41–Ru4	179 (1)
S–Ru1–Ru4	54.58 (5)	O42–C42–Ru4	158.7 (8)
S–Ru1–Ru3	54.58 (5)	O43–C43–Ru4	177.0 (7)
S–Ru1–Mo1	80.23 (5)	O51–C51–Mo1	160.7 (8)
Ru2–Ru1–Ru4	146.85 (3)	O61–C61–Mo2	160.5 (7)
Ru2–Ru1–Ru3	58.17 (2)	O62–C62–Mo2	155.9 (7)
Ru2–Ru1–Mo1	96.04 (3)	Mo2–Ru3–Mo1	65.37 (3)
Ru4–Ru1–Ru3	88.83 (3)	C41–Ru4–Ru1	134.1 (3)
Ru4–Ru1–Mo1	60.02 (2)	C41–Ru4–Mo2	114.2 (3)
Ru3–Ru1–Mo1	58.68 (2)	C41–Ru4–Mo1	93.4 (3)
C21–Ru2–Ru3	89.0 (3)	C43–Ru4–Ru1	128.4 (3)
C21–Ru2–Ru1	94.6 (3)	C43–Ru4–Mo2	91.0 (2)
C23–Ru2–Ru3	105.1 (3)	C43–Ru4–Mo1	154.7 (3)
C23–Ru2–Ru1	165.9 (3)	C42–Ru4–Ru1	61.3 (3)
C22–Ru2–Ru3	161.1 (3)	C42–Ru4–Mo2	150.4 (3)
C22–Ru2–Ru1	97.9 (3)	C42–Ru4–Mo1	108.0 (3)
O24–Ru2–Ru3	76.4 (1)	S–Ru4–Ru1	53.71 (5)
O24–Ru2–Ru1	76.4 (1)	S–Ru4–Mo2	52.78 (5)
Ru3–Ru2–Ru1	63.25 (2)	S–Ru4–Mo1	81.59 (5)
C32–Ru3–Ru2	86.3 (3)	Ru1–Ru4–Mo2	91.68 (3)
C32–Ru3–Ru1	132.8 (3)	Ru1–Ru4–Mo1	63.05 (2)
C32–Ru3–Mo2	120.2 (3)	Mo2–Ru4–Mo1	64.68 (2)
C32–Ru3–Mo1	96.7 (2)	C24–Mo1–Ru3	51.3 (2)
C31–Ru3–Ru2	94.8 (2)	C24–Mo1–Ru4	106.7 (2)
C31–Ru3–Ru1	119.1 (2)	C24–Mo1–Ru1	50.0 (2)
C31–Ru3–Mo2	98.3 (2)	C24–Mo1–Mo2	107.6 (2)
C31–Ru3–Mo1	163.6 (2)	C51–Mo1–Ru3	123.0 (3)
C24–Ru3–Ru2	58.8 (2)	C51–Mo1–Ru4	60.9 (3)
C24–Ru3–Ru1	52.1 (2)	C51–Mo1–Ru1	65.0 (3)
C24–Ru3–Mo2	106.5 (2)	C51–Mo1–Mo2	117.7 (3)
C24–Ru3–Mo1	42.1 (2)	C71–Mo1–Ru3	143.7 (2)
S–Ru3–Ru2	101.14 (5)	C71–Mo1–Ru4	127.8 (2)
S–Ru3–Ru1	53.27 (5)	C71–Mo1–Ru1	127.1 (2)
S–Ru3–Mo2	52.75 (5)	C71–Mo1–Mo2	147.3 (2)
S–Ru3–Mo1	82.39 (5)	C72–Mo1–Ru3	109.5 (2)
Ru2–Ru3–Ru1	58.58 (3)	C72–Mo1–Ru4	161.5 (3)
Ru2–Ru3–Mo2	149.75 (3)	C72–Mo1–Ru1	123.5 (2)
Ru2–Ru3–Mo1	99.52 (3)	C72–Mo1–Mo2	139.5 (3)
Ru1–Ru3–Mo2	91.30 (3)	C75–Mo1–Ru3	150.6 (2)
Ru1–Ru3–Mo1	63.39 (2)	C75–Mo1–Ru4	111.4 (2)
C61Mo2–Mo1	62.8 (2)	C75–Mo1–Ru1	151.5 (2)
C62–Mo2–Ru3	57.8 (2)	C75–Mo1–Mo2	112.3 (2)
C62–Mo2–Ru4	125.1 (2)	C73–Mo1–Ru3	96.4 (2)
C62–Mo2–Mo1	67.0 (2)	C73–Mo1–Ru4	155.8 (2)
S–Mo2–Ru3	54.33 (5)	C73–Mo1–Ru1	143.0 (2)
S–Mo2–Ru4	53.91 (5)	C73–Mo1–Mo2	104.9 (2)
S–Mo2–Mo1	78.38 (5)	C74–Mo1–Ru3	116.1 (2)
Ru3–Mo2–Ru4	87.47 (3)	C74–Mo1–Ru4	123.8 (2)
Ru3–Mo2–Mo1	57.35 (2)	C74–Mo1–Ru1	173.9 (2)
Ru4–Mo2–Mo1	58.38 (2)	C74–Mo1–Mo2	91.6 (2)
Mo2–S–Ru1	117.31 (8)	Ru3–Mo1–Ru4	86.56 (3)
Mo2–S–Ru4	73.31 (6)	Ru3–Mo1–Ru1	57.93 (2)
Mo2–S–Ru3	72.92 (6)	Ru3–Mo1–Mo2	57.29 (2)
Ru1–S–Ru4	71.71 (6)	Ru4–Mo1–Ru1	56.93 (2)
Ru1–S–Ru3	72.15 (6)	Ru4–Mo1–Mo2	56.93 (2)
Ru4–S–Ru3	109.46 (8)	Ru1–Mo1–Mo2	84.08 (3)
C24–O24–Ru2	90.0 (4)	C61–Mo2–Ru3	119.9 (2)
O11–C11–Ru1	178.4 (9)	C61–Mo2–Ru4	65.3 (2)

Description of the Structure of $Mo_2Ru_4(CO)_{14}Cp_2(\mu_4\text{-}S)$ (3). An ORTEP drawing of the molecular structure of **3** is shown in Figure 2. Final atomic positional parameters are listed in Table V. Intramolecular bond distances and angles are listed in Tables VI and VII, respectively. The molecule consists of a square-pyramidal cluster of one molybdenum and four ruthenium atoms

Table V. Positional Parameters and B(eq) for $Mo_2Ru_4(CO)_{14}Cp_2(\mu_4\text{-}S)$ (**3**)

atom	x	y	z	B(eq), Å^2
Ru1	0.33129 (11)	0.160812 (86)	0.14247 (14)	2.12 (9)
Ru2	0.25515 (10)	0.159652 (85)	−0.03725 (12)	1.81 (9)
Ru3	0.19090 (10)	0.127974 (79)	0.13784 (13)	1.66 (8)
Ru4	0.361948 (95)	0.075197 (82)	0.00082 (15)	2.06 (8)
Mo1	0.220393 (99)	0.32120 (79)	−0.00239 (15)	1.57 (8)
Mo2	0.11248 (11)	0.120621 (85)	−0.04176 (14)	1.8 (1)
S	0.28615 (31)	0.05581 (25)	0.13709 (39)	1.8 (3)
O11	0.42947 (94)	0.14070 (74)	0.3100 (13)	4.4 (4)
O12	0.36321 (98)	0.29487 (5)	0.1389 (12)	4.6 (4)
O13	0.23938 (89)	0.20276 (69)	0.3050 (11)	3.4 (4)
O14	0.48243 (99)	0.14991 (81)	0.0680 (12)	4.4 (4)
O21	0.20177 (92)	0.28065 (77)	0.0272 (12)	4.3 (4)
O22	0.21370 (87)	0.16477 (70)	−0.2497 (12)	3.7 (4)
O23	0.38454 (99)	0.22656 (75)	−0.1046 (13)	4.7 (4)
O31	0.0833 (10)	0.22355 (77)	0.1816 (13)	4.8 (4)
O32	0.11131 (92)	0.05929 (70)	0.2876 (11)	3.7 (4)
O41	0.44058 (99)	0.08468 (79)	−0.1868 (13)	4.9 (4)
O42	0.4366 (11)	−0.04086 (93)	0.0513 (15)	6.1 (5)
O51	0.28569 (81)	0.04312 (62)	−0.2027 (10)	2.5 (3)
O61	0.03381 (83)	0.02858 (65)	0.0898 (11)	2.9 (3)
O62	0.11758 (89)	0.02926 (68)	−0.2065 (11)	3.5 (4)
C11	0.3904 (13)	0.1487 (11)	0.2453 (19)	3.3 (5)
C12	0.3532 (11)	0.24172 (97)	0.1384 (16)	2.3 (5)
C13	0.2501 (14)	0.1793 (10)	0.2334 (17)	3.2 (5)
C14	0.4273 (13)	0.1320 (11)	0.0628 (17)	3.2 (5)
C21	0.2201 (13)	0.2327 (10)	0.0051 (18)	3.0 (5)
C22	0.2241 (12)	0.16277 (97)	−0.1668 (16)	2.4 (5)
C23	0.3390 (13)	0.2005 (11)	−0.0754 (16)	2.8 (5)
C31	0.1236 (14)	0.1879 (11)	0.1564 (18)	3.6 (6)
C32	0.1416 (12)	0.08496 (94)	0.2294 (16)	2.4 (5)
C41	0.4113 (14)	0.0803 (11)	−0.1164 (18)	3.3 (5)
C42	0.4092 (14)	0.0044 (12)	0.0350 (18)	3.7 (6)
C51	0.2706 (12)	0.05112 (92)	−0.1200 (15)	1.9 (5)
C61	0.0686 (11)	0.06097 (94)	0.0421 (16)	1.9 (4)
C62	0.1235 (12)	0.06034 (92)	−0.1362 (16)	2.3 (5)
C71	0.2388 (12)	−0.06537 (96)	0.0682 (15)	2.3 (5)
C72	0.1687 (12)	−0.05329 (92)	0.0722 (15)	1.8 (4)
C73	0.1421 (11)	−0.05011 (90)	−0.0256 (15)	1.9 (4)
C74	0.2002 (12)	−0.0591 (10)	−0.0849 (15)	2.3 (5)
C75	0.2581 (12)	−0.06843 (93)	−0.0259 (15)	2.2 (5)
C81	0.0020 (15)	0.1665 (11)	−0.0230 (18)	4.1 (6)
C82	0.0506 (13)	0.2140 (10)	−0.0309 (17)	3.0 (5)
C83	0.0787 (14)	0.2129 (10)	−0.1199 (18)	3.2 (5)
C84	0.0522 (12)	0.1645 (10)	−0.1708 (16)	2.5 (5)
C85	0.0062 (13)	0.1335 (10)	−0.1083 (17)	2.8 (5)

Table VI. Intramolecular Distances (Å) for $Mo_2Ru_4(CO)_{14}Cp_2(\mu_4\text{-}S)$ (**3**)

Ru1–C12	1.82 (2)	Ru4–C42	1.86 (3)
Ru1–C11	1.85 (3)	Ru4–C41	1.89 (3)
Ru1–C13	2.05 (3)	Ru4–C14	1.97 (3)
Ru1–C14	2.25 (2)	Ru4–S	2.433 (6)
Ru1–S	2.459 (6)	Ru4–Mo1	2.871 (3)
Ru1–Ru4	2.788 (3)	Mo1–C51	1.95 (2)
Ru1–Ru3	2.792 (3)	Mo1–C75	2.34 (2)
Ru1–Ru2	2.905 (3)	Mo1–C74	2.34 (2)
Ru2–C21	1.83 (2)	Mo1–C72	2.36 (2)
Ru2–C22	1.91 (2)	Mo1–C73	2.37 (2)
Ru2–C23	1.92 (3)	Mo1–S	2.375 (6)
Ru2–Ru4	2.813 (3)	Mo1–C71	2.38 (2)
Ru2–Ru3	2.825 (3)	Mo1–Mo2	2.896 (3)
Ru2–Mo2	2.871 (3)	Mo2–C62	1.88 (2)
Ru2–Mo1	2.911 (3)	Mo2–C61	1.95 (2)
Ru3–C32	1.85 (2)	Mo2–C85	2.26 (2)
Ru3–C31	1.86 (3)	Mo2–C84	2.35 (2)
Ru3–C13	2.08 (2)	Mo2–C81	2.36 (3)
Ru3–S	2.418 (6)	Mo2–C82	2.37 (2)
Ru3–Mo1	2.928 (3)	Mo2–C83	2.39 (2)
Ru3–Mo2	2.930 (3)		

with one molybdenum atom Mo2 capping the Mo1, Ru2, Ru3 triangular face and a quadruply bridging sulfido ligand spanning the square base. In contrast to **2**, a ruthenium atom occupies the apical position in the square pyramid. The Mo–Mo distance of

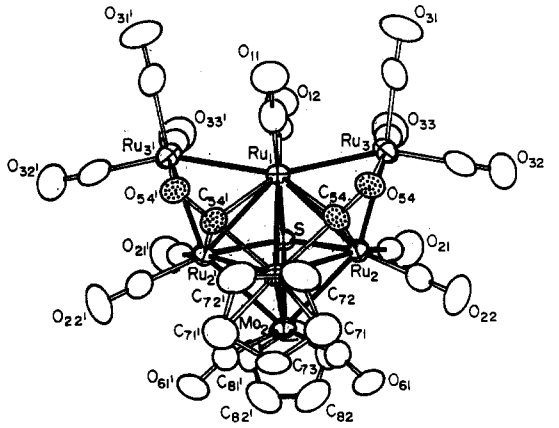

Figure 3. ORTEP diagram of $Mo_2Ru_5(CO)_{14}(\mu_4\text{-}\eta^2\text{-}CO)_2Cp_2(\mu_4\text{-}S)$ (**4**), showing 50% probability thermal ellipsoids.

2.896 (3) Å is significantly shorter than that in **1**, 3.0282 (8) Å.[11] All the Mo–Ru distances lie in a fairly narrow range, 2.871 (3)–2.930 (3) Å. Except for the Ru1–Ru2 distance of 2.905 (3) Å, all the Ru–Ru bonds are very similar in length, 2.788 (3)–2.825 (3) Å. The metal–sulfur distances are similar to those observed in **2** and **5**. Compound **3** contains 14 carbonyl ligands distributed about the cluster as shown in Figure 2. Eleven of these are normal terminally coordinated ligands. C13–O13 and C14–O14 are normal edge-bridging ligands, and C51–O51 is a semibridge. The η^5-cyclopentadienyl ligands exhibit no unusual bonding distortions. Compound **3** contains a total of 88 cluster valence electrons. This is in accord with the count predicted by the PSEP theory for a capped octahedron in which one of the cluster atoms is a main-group element.

Description of the Structure of $Mo_2Ru_5(CO)_{14}(\mu_4\text{-}\eta^2\text{-}CO)_2Cp_2(\mu_4\text{-}S)$ (4). An ORTEP drawing of **4** is shown in Figure 3. Final atomic positional parameters are listed in Table VIII. Interatomic distances and angles are listed in Tables IX and X, respectively. The compound crystallized in the monoclinic space group $P2_1/m$ with two formula equivalents in the unit cell. The structural analysis showed that the molecular unit thus contains a crystallographically imposed reflection plane. Figure 3 shows both halves of the molecule. The atoms Mo1, Mo2, Ru1, S, C11, O11, C12, O12, C73, and C83 all lie on this reflection plane. The complete molecule consists of a square-pyramidal Mo_2Ru_3 cluster that is very similar to **2**. Like **2**, compound **4** also contains a $Ru(CO)_3$ group bridging one Ru–Ru basal edge of the square pyramid, but unlike **2**, it also contains a second such bridging group across the second Ru–Ru basal edge of the square pyramid. The metal–metal bonding in **4** is virtually the same as that in **2** with two exceptions. The Mo1–Ru1 bond, 2.918 (2) Å in **4**, is significantly shorter than that in **2**, 3.022 (1) Å, and the Ru1–Ru3 bond, 2.800 (1) Å in **4**, is significantly longer than the corresponding distance in **2**, 2.737 (1) Å. The lengthening of the Ru1–Ru3 bond in **4** may be influenced by the Ru1–Ru3′ bond trans to it, which is absent in **2**.

Compound **4** contains two quadruply bridging carbonyl ligands and is the first example of such a molecule. The ligands are coordinated in the type F mode analogous to the one in **2**, and the C–O distance is elongated, 1.25 (1) Å. The two ligands are related by the reflection plane and are thus chemically equivalent; however, the infrared spectrum shows two absorptions, 1453 and 1419 cm^{-1}, in the region for the C–O stretching vibration (see Figure 4). It is believed that the splitting of the absorption is due to a vibrational coupling of the two ligands and leads to symmetric and antisymmetric modes. If the coupling mechanism is similar to that in other carbonyl complexes, the higher frequency absorption will be due to the symmetric stretch.[17] All of the remaining CO ligands in **4** are of a linear terminal type, except for C61–O61 (C61–O61′), which is a weak semibridge from Mo2

(17) Cotton, F. A.; Kraihanzel, C. S. *J. Am. Chem. Soc.* **1962**, *84*, 4432.

Table VII. Intramolecular Bond Angles (deg) for $Mo_2Ru_4(CO)_{14}Cp_2(\mu_4\text{-}S)$ (3)

C12-Ru1-Ru4	125.7 (7)	Mo2-Ru2-Mo1	60.11 (6)	C51-Mo1-Ru2	62.8 (6)	C85-Mo2-Ru3	144.0 (6)
C12-Ru1-Ru3	118.3 (7)	Ru1-Ru2-Mo1	88.75 (7)	C51-Mo1-Ru3	120.5 (6)	C84-Mo2-Ru2	111.4 (6)
C12-Ru1-Ru2	95.6 (7)	C32-Ru3-Ru1	127.6 (7)	C75-Mo1-Ru4	91.3 (6)	C84-Mo2-Mo1	140.7 (5)
C11-Ru1-Ru4	108.9 (8)	C32-Ru3-Ru2	161.3 (6)	C75-Mo1-Mo2	145.5 (5)	C84-Mo2-Ru3	152.6 (5)
C11-Ru1-Ru3	125.0 (8)	C32-Ru3-Mo1	101.4 (6)	C75-Mo1-Ru2	144.1 (5)	C81-Mo2-Ru2	136.7 (6)
C11-Ru1-Ru2	168.1 (8)	C32-Ru3-Mo2	107.5 (7)	C75-Mo1-Ru3	146.0 (5)	C81-Mo2-Mo1	155.3 (6)
C13-Ru1-Ru4	137.1 (7)	C31-Ru3-Ru1	119.1 (8)	C74-Mo1-Ru4	116.6 (6)	C81-Mo2-Ru3	110.1 (6)
C13-Ru1-Ru3	48.0 (7)	C31-Ru3-Ru2	104.5 (8)	C74-Mo1-Mo2	110.9 (6)	C82-Mo2-Ru2	102.7 (6)
C13-Ru1-Ru2	98.9 (7)	C31-Ru3-Mo1	137.3 (8)	C74-Mo1-Ru2	140.8 (5)	C82-Mo2-Mo1	157.8 (6)
C14-Ru1-Ru4	44.4 (6)	C31-Ru3-Mo2	78.5 (8)	C74-Mo1-Ru3	155.3 (6)	C82-Mo2-Ru3	99.0 (6)
C14-Ru1-Ru3	135.2 (6)	C13-Ru3-Ru1	47.0 (7)	C72-Mo1-Ru4	130.8 (5)	C83-Mo2-Ru2	91.0 (6)
C14-Ru1-Ru2	89.0 (6)	C13-Ru3-Ru2	100.6 (7)	C72-Mo1-Mo2	108.0 (5)	C83-Mo2-Mo1	148.1 (6)
S-Ru1-Ru4	54.8 (1)	C13-Ru3-Mo1	135.1 (7)	C72-Mo1-Ru2	158.3 (5)	C83-Mo2-Ru3	119.0 (6)
S-Ru1-Ru3	54.4 (1)	C13-Ru3-Mo2	149.2 (6)	C72-Mo1-Ru3	101.0 (5)	Ru2-Mo2-Mo1	60.62 (7)
S-Ru1-Ru2	77.8 (1)	S-Ru3-Ru1	55.8 (1)	C73-Mo1-Ru4	148.5 (5)	Ru2-Mo2-Ru3	58.28 (7)
Ru4-Ru1-Ru3	90.82 (8)	S-Ru3-Ru2	80.0 (1)	C73-Mo1-Mo2	91.4 (5)	Mo1-Mo2-Ru3	60.33 (7)
Ru4-Ru1-Ru2	59.18 (7)	S-Ru3-Mo1	51.7 (1)	C73-Mo1-Ru2	148.2 (5)	Mo1-S-Ru3	75.3 (2)
Ru3-Ru1-Ru2	59.43 (7)	S-Ru3-Mo2	110.5 (2)	C73-Mo1-Ru3	120.7 (5)	Mo1-S-Ru4	73.3 (2)
C21-Ru2-Ru4	141.3 (8)	Ru1-Ru3-Ru2	62.27 (7)	S-Mo1-Ru4	54.3 (1)	Mo1-S-Ru1	114.6 (2)
C21-Ru2-Ru3	77.0 (8)	Ru1-Ru3-Mo1	90.61 (8)	S-Mo1-Mo2	112.9 (2)	Ru3-S-Ru4	110.0 (2)
C21-Ru2-Mo2	85.2 (7)	Ru1-Ru3-Mo2	122.0 (1)	S-Mo1-Ru2	78.9 (1)	Ru3-S-Ru1	69.8 (2)
C21-Ru2-Ru1	84.2 (8)	Ru2-Ru3-Mo1	60.76 (7)	S-Mo1-Ru3	53.0 (2)	Ru4-S-Ru1	69.5 (2)
C21-Ru2-Mo1	134.4 (7)	Ru2-Ru3-Mo2	59.83 (7)	C71-Mo1-Ru4	98.7 (6)	O11-C11-Ru1	179 (2)
C22-Ru2-Ru4	115.5 (7)	Mo1-Ru3-Mo2	59.26 (7)	C71-Mo1-Mo2	141.7 (6)	O12-C12-Ru1	175 (2)
C22-Ru2-Ru3	133.9 (7)	C42-Ru4-Ru1	118.8 (8)	C71-Mo1-Ru2	153.9 (6)	O13-C13-Ru1	140 (2)
C22-Ru2-Mo2	72.0 (7)	C42-Ru4-Ru2	162.4 (8)	C71-Mo1-Ru3	113.3 (5)	O13-C13-Ru3	135 (2)
C22-Ru2-Ru1	167.8 (7)	C42-Ru4-Mo1	101.0 (8)	Ru4-Mo1-Mo2	117.48 (9)	Ru1-C13-Ru3	85 (1)
C22-Ru2-Mo1	97.0 (7)	C41-Ru4-Ru1	132.8 (7)	Ru4-Mo1-Ru2	58.21 (6)	O14-C14-Ru4	148 (2)
C23-Ru2-Ru4	75.3 (7)	C41-Ru4-Ru2	99.4 (8)	Ru4-Mo1-Ru3	86.52 (8)	O14-C14-Ru1	130 (2)
C23-Ru2-Ru3	136.2 (7)	C41-Ru4-Mo1	118.5 (8)	Mo2-Mo1-Ru2	59.27 (7)	Ru4-C14-Ru1	83 (1)
C23-Ru2-Mo2	159.1 (7)	C14-Ru4-Ru1	53.0 (7)	Mo2-Mo1-Ru3	60.41 (7)	O21-C21-Ru2	175 (2)
C23-Ru2-Ru1	79.2 (7)	C14-Ru4-Ru2	97.7 (7)	Ru2-Mo1-Ru3	57.88 (6)	O22-C22-Ru2	172 (2)
C23-Ru2-Mo1	133.2 (7)	C14-Ru4-Mo1	144.8 (7)	C62-Mo2-Ru2	96.7 (7)	O23-C23-Ru2	173 (2)
Ru4-Ru2-Ru3	89.64 (7)	S-Ru4-Ru1	55.7 (1)	C62-Mo2-Mo1	65.3 (7)	C31-C31-Ru3	170 (2)
Ru4-Ru2-Mo2	120.30 (9)	S-Ru4-Ru2	80.0 (1)	C62-Mo2-Ru3	125.6 (7)	O32-C32-Ru3	178 (2)
Ru4-Ru2-Ru1	58.35 (7)	S-Ru4-Mo1	52.4 (1)	C61-Mo2-Ru2	126.9 (6)	O41-C41-Ru4	178 (2)
Ru4-Ru2-Mo1	60.19 (7)	Ru1-Ru4-Ru2	62.47 (7)	C61-Mo2-Mo1	75.4 (6)	O42-C42-Ru4	176 (2)
Ru3-Ru2-Mo2	61.89 (7)	Ru1-Ru4-Mo1	91.87 (8)	C61-Mo2-Ru3	75.2 (6)	O51-C51-Mo1	154 (2)
Ru3-Ru2-Ru1	58.30 (7)	Ru2-Ru4-Mo1	61.60 (7)	C85-Mo2-Ru2	146.5 (6)	O61-C61-Mo2	171 (2)
Ru3-Ru2-Mo1	61.36 (6)	C51-Mo1-Ru4	58.6 (6)	C85-Mo2-Mo1	144.1 (6)	O62-C62-Mo2	164 (2)
Mo2-Ru2-Ru1	120.14 (9)	C51-Mo1-Mo2	92.9 (6)				

Scheme I

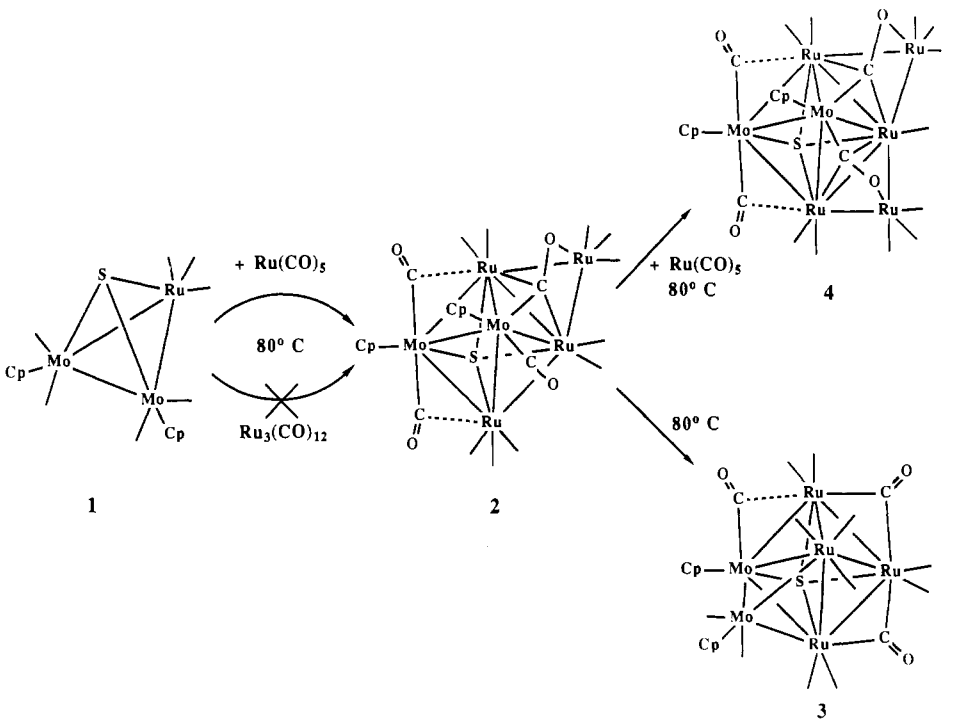

to Ru2 (Ru2'), Ru2···C61 = 2.71 (1) Å. If one assumes that each quadruply bridging carbonyl ligand serves as a four-electron donor, then compound **4** contains 104 cluster valence electrons. This is the number predicted by the PSEP theory for an octahedral cluster containing one main-group-element atom and two edge-bridging metal carbonyl groupings.

Table VIII. Positional Parameters and B(eq) for $Mo_2Ru_5(CO)_{14}(\mu_4\text{-}\eta^2\text{-}CO)_2Cp_2(\mu_4\text{-}S)$ (**4**)

atom	x	y	z	B(eq), Å^2
Ru1	0.716 338 (99)	1/4	0.65250 (13)	2.26 (5)
Ru2	0.803 202 (69)	0.119 366 (55)	0.518883 (91)	2.31 (3)
Ru3	0.688 274 (76)	0.070 673 (61)	0.68212 (10)	2.97 (4)
Mo1	0.653 60 (10)	1/4	0.34206 (13)	2.22 (5)
Mo2	0.899 05 (10)	1/4	0.39320 (13)	2.25 (5)
S	0.898 26 (29)	1/4	0.63285 (37)	2.2 (1)
O11	0.494 4 (10)	1/4	0.6853 (15)	5.5 (7)
O12	0.838 4 (12)	1/4	0.9721 (13)	5.5 (7)
O21	1.015 01 (70)	0.026 05 (65)	0.6946 (10)	5.9 (5)
O22	0.716 92 (77)	−0.037 66 (59)	0.3312 (10)	5.6 (4)
O31	0.540 39 (84)	0.043 64 (70)	0.8548 (11)	6.9 (5)
O32	0.700 39 (80)	−0.121 76 (62)	0.6318 (11)	5.9 (5)
O33	0.897 41 (78)	0.054 90 (72)	0.9411 (11)	6.3 (5)
O54	0.564 58 (55)	0.100 64 (47)	0.47986 (74)	3.0 (3)
O61	0.782 65 (65)	0.107 98 (54)	0.16728 (83)	3.8 (4)
C11	0.577 8 (13)	1/4	0.6720 (19)	3.7 (7)
C12	0.790 1 (14)	1/4	0.8505 (18)	3.4 (7)
C21	0.936 93 (95)	0.060 27 (78)	0.6299 (12)	3.4 (5)
C22	0.748 15 (92)	0.020 58 (81)	0.4017 (13)	3.4 (5)
C31	0.589 4 (10)	0.055 74 (76)	0.7860 (14)	4.1 (5)
C32	0.694 7 (11)	−0.051 49 (94)	0.6488 (14)	4.3 (6)
C33	0.819 4 (11)	0.061 22 (85)	0.8451 (15)	4.3 (6)
C54	0.630 02 (77)	0.153 71 (69)	0.4592 (10)	2.5 (4)
C61	0.812 55 (83)	0.157 39 (74)	0.2602 (12)	3.0 (5)
C71	0.548 44 (92)	0.175 49 (84)	0.1320 (11)	3.9 (5)
C72	0.481 01 (86)	0.204 65 (76)	0.2020 (11)	3.7 (5)
C73	0.590 4 (13)	1/4	0.0906 (15)	3.4 (7)
C81	1.064 55 (97)	0.178 47 (80)	0.4361 (17)	4.5 (6)
C82	1.024 9 (10)	0.206 10 (89)	0.2941 (16)	5.4 (7)
C83	1.087 6 (13)	1/4	0.5222 (17)	4.5 (9)
C91	0.284 8 (11)	0.206 38 (87)	−0.1227 (15)	5.8 (3)
C92	0.217 4 (13)	0.163 4 (11)	−0.0699 (17)	7.3 (4)
C93	0.147 9 (14)	0.209 2 (10)	−0.0181 (18)	8.1 (5)

Table IX. Intramolecular Distances (Å) for $Mo_2Ru_5(CO)_{14}(\mu_4\text{-}\eta^2\text{-}CO)_2Cp_2(\mu_4\text{-}S)$ (**4**)

Ru-C12	1.86 (2)	Mo2-C61	1.99 (1)
Ru1-C11	1.89 (2)	Mo2-C81	2.31 (1)
Ru1-C54	2.36 (1)	Mo2-C82	2.31 (1)
Ru1-S	2.453 (4)	Mo2-C83	2.32 (2)
Ru1-Ru3	2.800 (1)	Mo2-S	2.413 (4)
Ru1-Ru2	2.867 (1)	O11-C11	1.14 (2)
Ru1-Mo1	2.918 (2)	O12-C12	1.15 (2)
Ru2-C22	1.89 (1)	O21-C21	1.12 (1)
Ru2-C21	1.91 (1)	O22-C22	1.12 (1)
Ru2-C54	2.18 (1)	O31-C31	1.12 (1)
Ru2-S	2.407 (2)	O32-C32	1.10 (1)
Ru2-Ru3	2.706 (1)	O33-C33	1.12 (1)
Ru2-Mo2	2.887 (1)	O54-C54	1.25 (1)
Ru2-Mo1	2.897 (1)	O61-C61	1.15 (1)
Ru3-C33	1.88 (1)	C71-C72	1.39 (2)
Ru3-C32	1.91 (1)	C71-C73	1.39 (1)
Ru3-C31	1.95 (1)	C81-C83	1.36 (2)
Ru3-O54	2.125 (7)	C81-C82	1.39 (2)
Mo1-C54	1.98 (1)	C91-C92	1.35 (2)
Mo1-C72	2.28 (1)	C92-C93	1.39 (2)
Mo1-C71	2.34 (1)	Ru3-C54	2.44 (1)
Mo1-C73	2.35 (1)	C54-C54′	2.95 (1)
Mo1-Mo2	3.049 (2)	Ru2-C61	2.71 (1)

Discussion

Compound **1** readily adds three and four ruthenium carbonyl groupings by reaction with $Ru(CO)_5$ at 80 °C to yield the new cluster complexes **2** and **4**, which contain one and two quadruply bridging carbonyl ligands, respectively (see Scheme I). Compound **4** was also obtained from **2** by a further reaction with $Ru(CO)_5$ under similar conditions. It thus appears that **2** is an intermediate in the formation of **4**. Since $Ru(CO)_5$ is known to transform into $Ru_3(CO)_{12}$ under mild thermal treatment and since the formation of **2** involves the addition of three ruthenium carbonyl groupings, the preparation of **2** from a reaction of **1** with $Ru_3(CO)_{12}$ was attempted. No **2** was obtained from this reaction at 80 °C although **4** was formed at higher reaction temperatures.[18] As a result, it is believed that **2** was formed by a sequence of additions of mononuclear fragments, probably initially in the form of $Ru(CO)_4$ groupings. Although no lower nuclearity clusters were

Table X. Intramolecular Bond Angles (deg) for $Mo_2Ru_5(CO)_{14}(\mu_4\text{-}\eta^2\text{-}CO)_2Cp_2(\mu_4\text{-}S)$ (**4**)

C12-Ru1-Ru3	85.5 (1)	C54-Mo1-Ru2	111.5 (3)
C12-Ru1-Ru2	111.3 (3)	C54-Mo1-Ru1	53.7 (3)
C12-Ru1-Mo1	166.4 (5)	C54-Mo1-Mo2	106.6 (3)
C11-Ru1-Ru3	79.69 (5)	C54-Mo1-Ru2	111.5 (3)
C11-Ru1-Ru2	127.5 (3)	C54-Mo1-Ru2	48.6 (3)
C11-Ru1-Mo1	102.2 (5)	C54-Mo1-Ru1	53.7 (3)
C54-Ru1-Ru3	131.1 (2)	C54-Mo1-Mo2	106.6 (3)
C54-Ru1-Ru2	48.0 (2)	C72-Mo1-Ru2	151.2 (3)
C54-Ru1-Mo1	42.4 (2)	C72-Mo1-Ru1	118.8 (3)
C54-Ru1-Ru3	55.6 (2)	C72-Mo1-Mo2	147.2 (3)
C54-Ru1-Ru2	48.0 (2)	C72-Mo1-Ru2	117.1 (3)
C54-Ru1-Mo1	42.4 (2)	C72-Mo1-Mo2	147.2 (3)
S-Ru1-Ru3	100.20 (3)	C71-Mo1-Ru2	157.6 (3)
S-Ru1-Ru2	53.12 (5)	C71-Mo1-Ru1	143.3 (3)
S-Ru1-Mo1	79.0 (1)	C71-Mo1-Mo2	112.3 (3)
Ru3-Ru1-Ru2	57.04 (3)	C73-Mo1-Ru2	123.2 (2)
Ru3-Ru1-Mo1	96.77 (3)	C73-Mo1-Ru1	176.1 (4)
Ru2-Ru1-Mo1	60.10 (3)	C73-Mo1-Mo2	96.2 (4)
C22-Ru2-Ru3	89.4 (3)	Ru2-Mo1-Ru2	87.30 (5)
C22-Ru2-Ru1	136.6 (3)	Ru2-Mo1-Ru1	59.07 (3)
C22-Ru2-Mo2	114.1 (3)	Ru2-Mo1-Mo2	58.02 (3)
C22-Ru2-Mo1	99.0 (4)	C61-Mo2-Ru2	124.0 (3)
C21-Ru2-Ru3	96.1 (3)	C61-Mo2-Mo1	65.7 (3)
C21-Ru2-Ru1	119.3 (3)	C61-Mo2-Ru2	64.6 (3)
C21-Ru2-Mo2	97.7 (3)	C81-Mo2-Ru2	140.5 (4)
C21-Ru2-Mo1	160.9 (3)	C81-Mo2-Mo1	151.7 (3)
C54-Ru2-Ru3	58.8 (3)	C82-Mo2-Ru2	151.8 (3)
C54-Ru2-Ru1	53.8 (3)	C82-Mo2-Mo1	142.8 (3)
C54-Ru2-Mo2	106.6 (3)	C83-Mo2-Ru2	107.3 (3)
C54-Ru2-Mo1	43.1 (3)	C83-Mo2-Mo1	157.7 (4)
S-Ru2-Ru3	104.10 (9)	S-Mo2-Ru2	53.12 (5)
S-Ru2-Ru1	54.61 (8)	S-Mo2-Mo1	77.0 (1)
S-Ru2-Mo2	53.32 (8)	Ru2-Mo2-Mo1	58.36 (3)
S-Ru2-Mo1	80.18 (8)	Ru2-S-Mo2	73.56 (9)
Ru3-Ru2-Ru1	60.24 (3)	Ru2-S-Ru1	72.27 (9)
Ru3-Ru2-Mo2	152.11 (4)	Mo2-S-Ru1	116.3 (1)
Ru3-Ru2-Mo1	99.42 (4)	O11-C11-Ru1	179 (2)
Ru1-Ru2-Mo2	91.87 (4)	O12-C12-Ru1	178 (2)
Ru1-Ru2-Mo1	60.84 (4)	O21-C21-Ru2	180 (1)
Mo2-Ru2-Mo1	63.62 (4)	O22-C22-Ru2	179 (1)
C33-Ru3-Ru2	91.2 (4)	O31-C31-Ru3	174 (1)
C33-Ru3-Ru1	93.2 (4)	O32-C32-Ru3	179 (1)
C32-Ru3-Ru2	95.3 (3)	O33-C33-Ru3	179 (1)
C32-Ru3-Ru1	157.9 (3)	O54-C54-Mo1	148.0 (8)
C31-Ru3-Ru2	169.1 (4)	O54-C54-Ru2	120.0 (7)
C31-Ru3-Ru1	108.1 (3)	O54-C54-Ru1	114.5 (7)
O54-Ru3-Ru2	75.8 (2)	Mo1-C54-Ru2	88.2 (4)
O54-Ru3-Ru1	76.7 (2)	Mo1-C54-Ru1	83.9 (4)
Ru2-Ru3-Ru1	62.72 (3)	Ru2-C54-Ru1	78.2 (3)
C54-Mo1-Ru2	48.6 (3)	O61-C61-Mo2	161.9 (9)

Figure 4. IR spectra of **2** (a) and **4** (b) in the region 1350–1550 cm^{-1}, taken in CH_2Cl_2 solvent.

(18) Adams, R. D.; Wang, J. G., unpublished results.

Scheme II

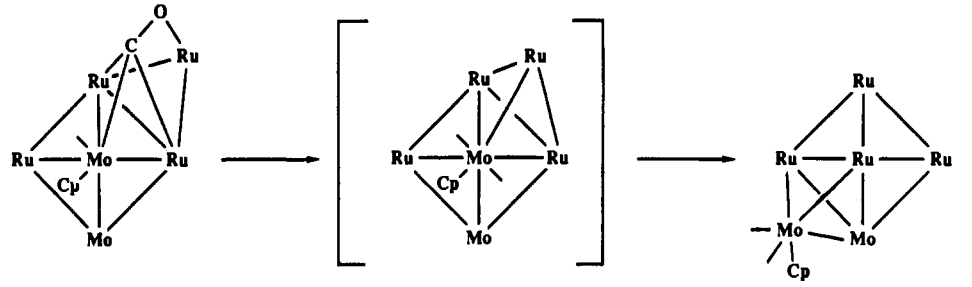

I

observed in these reactions, a logical precursor to **2** would be $Mo_2Ru_3(CO)_{12}Cp_2(\mu_4\text{-}S)$ (H), an isomer of **5** formed by the

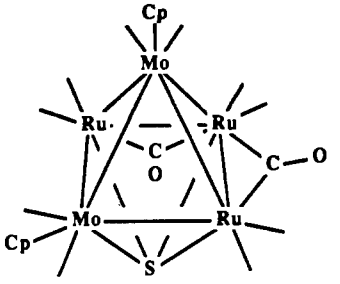

H

addition and insertion of two $Ru(CO)_4$ groupings into the metal–sulfur bonds of **1**. H contains a $CpMo(CO)_2$ group in the apical site of the square-pyramidal cluster. It is believed that the formation of **2** with the quadruply bridging carbonyl ligand then occurs by an interaction (e.g. type C) of a $Ru(CO)_4$ group with an oxygen atom of one of the bridging carbonyl ligands or one of the terminal ligands on the apical $CpMo(CO)_2$ group. CO elimination would lead to metal–metal bond formation. The fact that **2** is thermally isomerized to **3** supports this idea and demonstrates that **2** with the quadruply bridging carbonyl ligand is formed early in the reaction sequence.

The formation of **4** from **2** probably occurs by a similar process. A $Ru(CO)_4$ group interacts with the oxygen atom of a CO ligand in **2**. The most likely candidate would be the semitriply bridging ligand C51–O51 (see Figure 1). CO elimination and metal–metal bond formation would lead directly to **4**.

Compound **2** was treated thermally in the hope that the quadruply bridging CO ligand might undergo a C–O bond scission, but the formation of **3**, an isomer of **2**, shows that this did not occur. Instead, the quadruply bridging carbonyl ligand was converted into a terminally coordinated ligand. This transformation demonstrates that even quadruply bridging carbonyl ligands can undergo bridge–terminal rearrangements although this one is not reversible, as observed in the numerous degenerate systems that have been studied by dynamical NMR methods.[19] The shift of the quadruply bridging carbonyl ligand to a terminal-bonding mode has an important effect on the metal–metal bonding and structure of the cluster. First and foremost, the metal atoms lose two valence electrons, and the cluster is transformed from a 90-electron species to an 88-electron species. The primary consequence is that the cluster must condense, and it does this by transforming from an edge-bridged square pyramid to a face-capped square pyramid. The product that one would expect from such a transformation should contain a $Ru(CO)_3$ grouping in the capping position (e.g. intermediate I in Scheme II). However, **3** contains a $CpMo(CO)_2$ group in a capping site. Evidently, species I, if formed, rapidly isomerizes to **3** under the reaction conditions, presumably by interchanging the Ru capping group with the $CpMo(CO)_2$ apex in I, although a more complex mechanism that would shift the basal $CpMo(CO)_2$ group into a capping site cannot be excluded at this time.

Acknowledgment. These studies were supported by the National Science Foundation under Grant CHE-8612862. NMR measurements were made on a Bruker AM-300 spectrometer purchased with funds from the National Science Foundation under Grant No. CHE-8411172.

Supplementary Material Available: For compounds **2–4**, tables of C–C and C–O distances, hydrogen atom positional parameters, and anisotropic thermal parameters (7 pages); tables of observed and calculated structure factor amplitudes (50 pages). Ordering information is given on any current masthead page.

(19) Adams, R. D.; Cotton, F. A. In *Dynamic Nuclear Magnetic Resonance Spectroscopy*; Jackman, L. M.; Cotton, F. A., Eds.; Academic: New York, 1975.